

PHOTOCATHODE LASER PULSE SHAPING FOR IMPROVED EMITTANCE

M. Kotur*, J. Andersson, M. Brandin, J. Björklund Svensson, F. Curbis, F. Lindau, R. Lindvall, E. Mansten, L. Isaksson, R. Svärd, S. Thorin, S. Werin
 MAX IV Laboratory, Lund University, Lund, Sweden

Abstract

We present a setup for producing and characterizing picosecond ultraviolet laser pulses for use in the MAX IV photocathode electron gun preinjector. Frequency-tripled laser pulses from a commercial laser system are shaped directly in the ultraviolet domain using a Fourier-domain pulse shaper. The pulses were characterized using a transient grating FROG. We discuss a proposed upgrade of the pulse shaper, as well as its limitations.

INTRODUCTION AND MOTIVATION

The MAX IV Laboratory is a synchrotron radiation facility. Its two storage rings reach electron energies of 1.5 and 3 GeV. In addition to the rings, the lab operates a short pulse facility [1], while a design study for a soft X-ray free electron laser (FEL) at 1-5nm is currently in progress. Both rings are injected by a full energy linac at 3 GeV [2]. The linac can use either a thermionic or a photocathode gun as a source of electrons, but only the photocathode gun can deliver the short electron bunches required for the short pulse facility and the possible future FEL. Our 1.6-cell, normal-conducting, BNL/SLAC-type photocathode gun [3] is operated at 2.9985 GHz. We make use of a polished copper cathode. An emittance-compensating solenoid is installed directly following the gun. The emittance requirement for the short pulse facility of 10 μm has already been met. The more stringent requirement for the free electron laser, of 0.4 μm , at a charge of 40 pC is likely to necessitate developments of both the gun laser and the electron gun itself. Preliminary simulations conducted in ASTRA [4] indicate that the emittance of a spatially relatively uniform electron bunch is dependent on the shape of the photocathode laser pulse. In the case of a flat-top pulse shape with a finite rise-time, decreasing the rise time was predicted to reduce the emittance by up to 25%.

Our laser pulses are produced by a commercial laser system, which is capable of outputting 9 mJ infrared pulses at 790 nm, with a bandwidth of 25 nm. The laser system specifications have been summarized in Table 1. The infrared pulses are frequency tripled in a pair of β -BBO crystals, yielding ultraviolet pulses at 262 nm, with a photon energy of 4.7 eV, and a spectral bandwidth of 1.6 nm. Table 2 lists the UV pulse properties. These pulses are normally stretched to a duration of about 1.4 ps using a prism stretcher, and subsequently stacked to a final pulse duration of either 3ps or 6ps using birefringent α -BBO crystals [5]. The pulse energy

is about 100 μJ on cathode. The laser setup is described in more detail in [6].

Table 1: IR Pulse Specifications

Parameter	Value
Central wavelength	790 nm
Bandwidth	25 nm
Pulse energy	9 mJ
Repetition rate	100 Hz

Table 2: UV Pulse Specifications

Parameter	Value
Central wavelength	262 nm
Bandwidth	1.6 nm
Pulse energy	1 mJ
Repetition rate	20 Hz

The stacked pulses are characterized using two-color cross-correlation, where the picosecond UV pulses are gated using the IR pulses that are left over from the tripling, whose duration is about 100 fs. The IR pulses themselves are independently characterized in a second harmonic generation frequency resolved optical gating (SHG FROG). The pulses have a double Gaussian longitudinal profile, with a rise time of about 1 ps.

In order to produce picosecond pulses with a closer to a flat-top shape, we direct our pulses through a 4-f pulse shaper (Fig. 1). The pulse is first spectrally dispersed using a diffraction grating. A lens is placed a focal f length away from the grating ($g=3846 \text{ mm}^{-1}$), collimating the dispersed beam, and focusing it in the Fourier plane a distance f away. A double knife edge in the Fourier plane can be used to cut out some of the spectral components, and acts as a simple amplitude mask. After the Fourier plane the setup is reversed, so the beam is first collimated by another lens and finally the spectral components are overlapped again using another

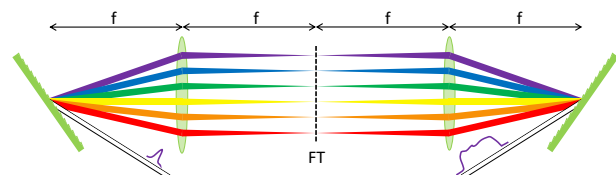


Figure 1: The principle of Fourier domain pulse shaping.

* marija.kotur@maxiv.lu.se

grating. Manipulating the different spectral components in the Fourier plane, e.g. by introducing either transparent or absorptive elements will modify the phase and/or the amplitude of the pulse, changing the temporal shape of the pulse at the output of the shaper. A deviation from the 4-f geometry would also lead to temporal reshaping the pulse. We make use of a commonly explored feature of imaging optical stretchers, where a translation of one of the gratings in the direction of the beam propagation leads to a quadratic phase being imparted on the pulse. This phase corresponds to a linear frequency chirp, which can be either positive or negative, depending on the direction in which the grating is moved.

The pulse shaper output is characterized using transient-grating frequency resolved optical gating (TG-FROG) [7]. The characterization setup is described in [6]. Directly after the frequency-tripling crystals, the UV pulses are close to transform limited with a pulse duration of about 80 fs, and an approximately Gaussian longitudinal profile.

RESULTS

Figure 2 demonstrates the possibilities for pulse shaping by adding quadratic phase through a modification in the pulse shaper geometry, in combination with simply cutting out the spectral components in the tails of the spectral intensity distribution. The added phase stretches the pulse, while the cutting the frequencies in the tails reduces the rise time of the final shape. Here we show the predicted and measured 3ps pulse.

The top panel shows the pulse in the spectral domain. A Gaussian with the FWHM of 1.6 nm is a good approximation for the measured spectrum, while a pure quadratic phase is assumed. The amplitude mask that was applied to the pulse is also shown. The middle panel shows the calculated temporal intensity and phase of the pulse. Here we also compare the resulting pulses with and without an amplitude mask applied. The effect of the mask is two-fold. While it does decrease the rise time of the pulse, it also introduces ringing in the amplitude, due to its sharp edges. The bottom panel shows the measured temporal shape of the pulse, which is in very good agreement with the calculated temporal shape. The temporal profile of a pulse produced through pulse stacking is plotted for comparison, and to highlight the improvement in the rise time.

In order to achieve a greater degree of control over the temporal shape of the pulse, we propose using a programmable device in the Fourier plane of the pulse shaper. A number of devices capable of shaping the electric field of a laser have been demonstrated, however only an acousto-optic modulator (AOM) can be used for the short wavelengths needed to photoionize a copper cathode [8, 9]. An AOM is essentially a programmable transmissive grating, consisting of a crystal and a piezo-electric transducer attached to it. Fused silica is commonly used at UV wavelengths. An RF wave sent to the piezo forms an acoustic wave in the crystal, resulting in a density and refractive index modulation. The device

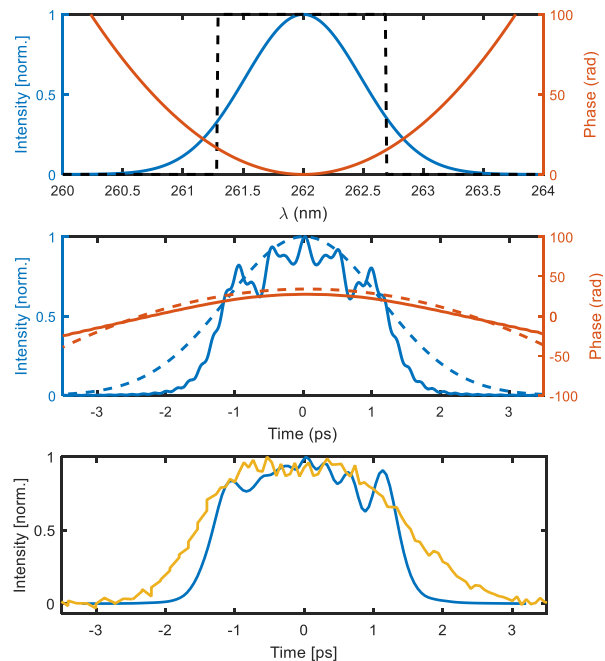


Figure 2: [Top panel] shaped laser pulse in the spectral domain: spectral intensity (solid blue), spectral phase (solid red), amplitude mask (dashed black). [Middle panel] shaped laser pulse in the temporal domain: temporal intensity with the amplitude mask applied (solid blue), and without the amplitude mask (dashed blue), temporal phase with the amplitude mask applied (solid red), and without the amplitude mask (dashed red). [Bottom panel] measured pulses, at the output of the pulse shaper (blue), stacked pulses (yellow).

allows for independent modification of the spectral phase and amplitude. It is worth noting that amplitude modification results in losses, while a smooth phase modification in principle does not.

The limitation in the phase variation rate an AOM can achieve is set by the pulse dispersion in the Fourier plane, as well as by the response of the AOM crystal itself. Commercially available AOM devices are typically operated at frequencies in the 100-200 MHz range. At the commercially available 3dB bandwidth of 100 MHz, the rise time is limited to 10ns. In our case, at $f=450$ mm, the spatial spread in the Fourier plane is 1.9 mm/nm and thus the slope of the phase variation rate is limited to about 100 rad/nm. This also limits the pulse duration that can be reached by applying only a quadratic phase to about 2 ps given our current optics and an input bandwidth of 1.6 nm. For this reason, we propose the use of a combined method. If the desired pulse shape is significantly longer than the input pulse, then the phase needed to achieve that pulse will have a large quadratic component. This component can be imparted on the pulse geometrically, i.e. by departing from the 4-f configuration. The pulse shaper is then only used for smaller adjustments in the pulse duration, as well as to shorten the rise time of the pulse.

Figure 3, top panel, shows a pulse shaped to produce a nearly flat-top distribution in the temporal domain. The phase need to achieve this is a sum of quadratic and a generalized Gaussian component, which are shown separately. The parameters of the generalized Gaussian were optimized in order to obtain the desired pulse shape. In addition, a smooth amplitude mask (a Tukey window) can be applied to the pulses. The bottom panel shows the same pulse in the temporal domain, including a comparison between the shapes obtained with (solid blue) and without (dashed blue) the phase mask. It is evident that applying a phase mask results in a reduction in the rise time, from about 0.7ps to 0.3ps. Using a smooth amplitude mask also reduces the ringing significantly. This highlights the clear advantages of using a fully controllable amplitude filter over a simple knife-edge

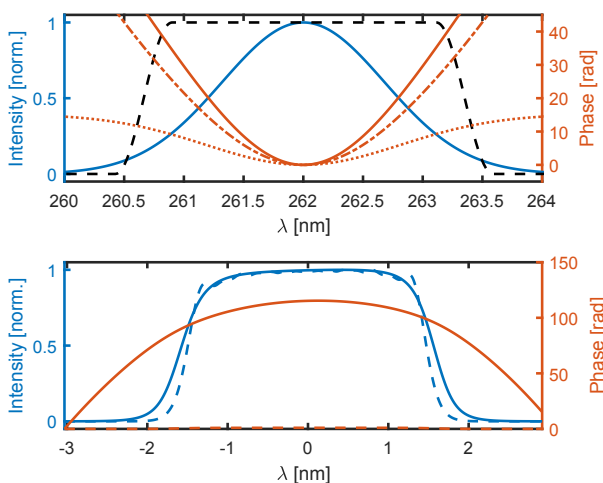


Figure 3: Top panel: a shaped laser pulse in the spectral domain. Here we show the spectral intensity (solid red) and the spectral phase (solid red). In addition, a the phase is decomposed into two components, a quadratic one (red dash-dotted line) and the remaining quasi-Gaussian (dotted red). A phase mask is shown (dashed black). Bottom panel: the same pulse in the temporal domain. We plot the temporal intensity corresponding to the pulse with a Gaussian spectrum (solid blue), and a temporal intensity corresponding to truncated Gaussian spectrum (dashed blue). The temporal phase is also shown (solid red).

CONCLUSION

We briefly present the laser setup used to produce femtosecond ultraviolet pulses. We discuss the different approaches to stretching and shaping these pulses. An existing setup consisting of a prism stretcher and birefringent crystals is compared with a newly built Fourier domain shaper. In addition, the use of a AOM device to improve the temporal shape is discussed, and simulated pulse shapes are presented.

REFERENCES

- [1] S. Werin *et al.*, “Short pulse facility for MAX-lab”, *Nucl. Instr. Meth. A*, vol. 601, pp. 98–107, 2009.
- [2] S. Thorin *et al.*, “The MAX IV Lina”, in *Proc. 27th Linear Accelerator Conf. (LINAC’14)*, Geneva, Switzerland, Aug.-Sep. 2014, paper TUIOA03, pp. 400–403.
- [3] M. Trovo *et al.*, “Status of the FERMI@ELETTRA photoinjector”, in *Proc. 11th European Particle Accelerator Conf. (EPAC’08)*, Genoa, Italy, Jun. 2008, pp. 247–249.
- [4] K. Floettmann, “ASTRA - A space charge tracking algorithm - DESY”, DESY, Hamburg, Germany, 2011.
- [5] J. G. Power *et al.*, “Temporal Laser Pulse Shaping for RF Photocathode Guns: The Cheap and Easy way using UV Birefringent Crystals”, in *Advanced Accelerator Concepts: Proc. 13th Advanced Accelerator Concepts Workshop*, Santa Cruz, CA, USA, Jul.-Aug. 2018, *AIP Conference Proceedings*, vol. 1086, pp. 689–694, 2009. doi:10.1063/1.3080991
- [6] F. Lindau, *et al.*, “MAXIV Photocathode Gun Laser System Specification and Diagnostics”, in *Proc. 8th Int. Particle Accelerator Conf. (IPAC’17)*, Copenhagen, Denmark, May 2017, pp. 1544–1546. doi:10.18429/JACoW-IPAC2017-TUPAB097
- [7] D. J. Kane *et al.*, “Characterization of arbitrary femtosecond pulses using frequency-resolved optical gating”, *IEEE J. Quant. Electron*, vol. 29, no. 2, p. 571, 1993.
- [8] A. M. Weiner *et al.*, “Femtosecond optical pulse shaping and processing”, in *Prog. Quantum Electron.*, vol. 19, pp. 161–237, 1995.
- [9] B. J. Pearson and T. C. Weinacht, “Shaped ultrafast laser pulses in the deep ultraviolet”, in *Opt. Express*, vol. 15, no. 7, pp. 4385–4388, 2007.